

Electrical Properties of the $\text{Cu}_2\text{O}/\text{Cd}_{1-x}\text{Zn}_x\text{Te}$ Heterostructure

E.V. Maistruk*, I.P. Koziarskyi, D.P. Koziarskyi, P.D. Maryanchuk

Yuriy Fedkovych Chernivtsi National University, 2, Kotsyubynsky St., 58012 Chernivtsi, Ukraine

(Received 27 November 2018; revised manuscript received 04 April 2019; published online 15 April 2019)

The work describes the influence of growth conditions on the optical and electrical properties of Cu_2O thin films. The electrical properties of the $p\text{-Cu}_2\text{O}/n\text{-Cd}_{1-x}\text{Zn}_x\text{Te}$ heterostructure obtained on the basis of these films were also investigated.

Cu_2O thin films were obtained by the method of RF magnetron sputtering of a target from copper oxide II powder on glass and glass-ceramic substrates. In the production of the films under study, the temperature of the substrates ($270^\circ\text{C} \leq T_s \leq 375^\circ\text{C}$) and the time of sputtering of the target ($30 \text{ min} \leq t \leq 60 \text{ min}$) were changed. By optimal conditions, $p\text{-Cu}_2\text{O}$ films were obtained with an optical band gap of $E_g^{\text{opt}} = 2.6 \text{ eV}$ and a specific resistance of $\rho = 0.5 \Omega \times \text{cm}$. The $p\text{-Cu}_2\text{O}/n\text{-Cd}_{1-x}\text{Zn}_x\text{Te}$ heterostructures were obtained using the RF magnetron sputtering of a target from copper oxide II powder on fresh-split $\text{Cd}_{1-x}\text{Zn}_x\text{Te}$ substrates. Investigation of the effect of temperature ($23^\circ\text{C} \leq T \leq 80^\circ\text{C}$) on the I - V -characteristics of $p\text{-Cu}_2\text{O}/n\text{-Cd}_{1-x}\text{Zn}_x\text{Te}$ heterostructures showed that the heterostructures have a pronounced rectifying effect with a rectification coefficient $RR \sim 10^3$ at a voltage of 2 V, the potential barrier height $e_{\text{ph}} = 0.77 \text{ eV}$ at $T = 296 \text{ K}$ and decreases with increasing temperature. The successive resistance of the heterostructures reaches $R_s \sim 500 \Omega$ at room temperature and is formed by the $n\text{-Cd}_{1-x}\text{Zn}_x\text{Te}$ substrates and decreases with increasing temperature. The study of current transfer mechanisms showed that, at small displacements, over-barrier emission prevails, at medium displacement, tunneling predominates, and at large displacements, the generation-recombination mechanism of current transfer with the participation of surface states on the metallurgical boundary separation. With increasing temperature, the generation-recombination mechanism of current transfer gradually disappears and passes into tunneling, which may be due to an increase in the concentration of electrons with a temperature rise in the base region of the heterojunction ($\text{Cd}_{1-x}\text{Zn}_x\text{Te}$) and a decrease in the potential barrier height.

Keywords: Thin films, Heterostructure, I - V -characteristics, Cu_2O , HF magnetron sputtering.

DOI: [10.21272/jnep.11\(2\).02007](https://doi.org/10.21272/jnep.11(2).02007)

PACS numbers: 73.61.Le, 81.15.Ef

1. INTRODUCTION

Copper oxide as a material of electrical engineering is used from the 20's to 30's of the last century. So, for example, on the basis of copper oxides, the first rectifier is built. But copper oxides as materials for solar power began to be widely discussed quite recently [1-3].

The main advantages of copper oxide films, as materials of electronics and solar energy, are their non-toxicity to humans, a large number of methods of obtaining, cheap copper due to its widespread distribution. In addition, copper oxides can be used in gas-sensitive sensors, lithium-ion batteries, photocells, and others.

In recent years, the main issue of extending the boundaries of the use of copper oxides in solar power and electronics is to improve the optical, electrical and structural characteristics of these oxides [4]. Their special value is: copper oxide strongly changes its properties (type of conductivity, width of the band gap) depending on the oxygen content [3].

Therefore, it was interesting to investigate the dependence of the electrical and optical properties of Cu_2O thin films on the technological regimes of their preparation by the method of RF magnetron sputtering [5]. In addition, a $p\text{-Cu}_2\text{O}/n\text{-Cd}_{1-x}\text{Zn}_x\text{Te}$ heterostructure was created and its electrical properties were investigated to establish the possibility of practical use of the obtained copper oxide films. Solid solutions $\text{Cd}_{1-x}\text{Zn}_x\text{Te}$ were chosen as the base substrate due to their higher

mechanical strength, structural perfection and value of band gap [6]. This makes them suitable for use in solar power cells.

2. EXPERIMENTAL METHOD

Cu_2O thin films were obtained by the method of RF magnetron sputtering of the CuO target. The sputtering process was carried out in the YBH-70 equipment, which for this purpose was equipped with a magnetron, whose operating frequency was 13.56 MHz. In order, to avoid getting sulfur from vacuum oil into the film, a turbomolecular pump TMH-500 was used as a high-vacuum pump. A copper oxide II powder was pressed into an aluminum cup to make the target. The internal diameter of the cup is considerably larger than the diameter of the eroding zone (working spray region) of the magnetron to prevent sputtering of the cup's material.

Thin films of Cu_2O were applied: on glass substrates (a cover glass was used as a substrate) to investigate the optical properties, on glass-ceramic substrates to investigate the electrical properties. The substrates were placed on a stainless steel stove, which allowed temperatures of up to 600°C to be maintained. The substrate temperature was controlled using K-thermocouple.

All films of Cu_2O were obtained at a magnetron power of 180 W. The process of film deposition lasted 30 and 60 minutes.

Cu_2O films were deposited on $n\text{-Cd}_{1-x}\text{Zn}_x\text{Te}$ fresh-split crystal plate to obtain heterostructures. These crystals were grown by Bridgman method [7, 8] and had a

* e.maistruk@chnu.edu.ua

specific resistance $\rho > 10^2$ Ohm. Their composition was controlled using Hall coefficient studies along the length of the crystal.

3. RESULTS AND DISCUSSION

3.1 Optical Properties of Cu₂O Thin Films

Investigation of optical coefficients was carried out with the help of the spectrophotometer CФ-2000 with spectral range of studies from 0.2 to 1.1 μm . The transmission spectra of thin films are presented in Fig. 1.

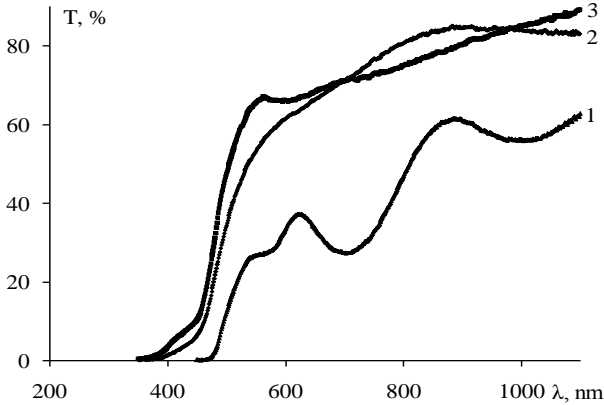


Fig. 1 – The transmission spectra of thin films Cu₂O: 1 – $t = 60$ min, $T_s = 315$ °C; 2 – $t = 30$ min, $T_s = 270$ °C; 3 – $t = 30$ min, $T_s = 375$ °C

A method based on the independent measurement of the reflection and transmission coefficient was used to determine the optical coefficients. The possibility of using this method to study the optical coefficients of semiconductor thin films deposited on a transparent substrate is justified in [19].

Thus, to measure the absorption coefficient (α), it was necessary to measure the transmission (T) and reflection (R) coefficients. Measurement of the reflection coefficient was performed using the CФ-2000 spectrometer and the Pike reflector measuring unit. To do this, a halogen lamp was used as a light source, which allowed to study reflection spectra in the wavelength range of $\lambda = 0.4\text{-}1.1$ μm .

In this case, the absorption coefficient can be calculated by the formula:

$$\alpha = \frac{1}{d} \ln \left[\frac{(1-R)^2}{2T} + \sqrt{\frac{(1-R)^4}{4T^2} + R^2} \right]$$

For the obtained Cu₂O films there were straight-line regions (Fig. 2) in the dependences $\alpha^2 = f(h\nu)$. This indicates that Cu₂O belongs to direct-band semiconductors and allowed to determine the width of the optical band gap for each sample.

The electrical resistance of the films was investigated by a four-probe method on a direct current. The thickness was measured using the Linnaek microinterferometer MIII-4.

The film thickness (d), the optical widths of the band gaps (E_g), the resistivity (ρ) [10] of the Cu₂O films obtained at different substrate temperatures (T_s) and the duration of the spray process (t) are given in Table 1.

The determined values of the band gap have allowed us to conclude that the films obtained are Cu₂O but not CuO. The optical band gap of the films obtained reached 2.5-2.58 eV, which is characteristic of Cu₂O. For CuO, the width of the band gap is within the range of 1.4-1.7 eV.

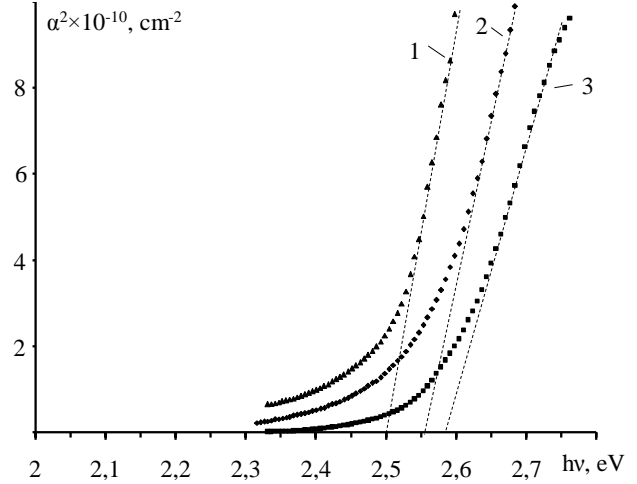


Fig. 2 – Absorption spectra of thin films Cu₂O: 1 – $t = 60$ min, $T_s = 315$ °C; 2 – $t = 30$ min, $T_s = 270$ °C; 3 – $t = 30$ min, $T_s = 375$ °C

Table 1 – Parameters of thin films Cu₂O

	t , min	T_s , °C	E_g , eV	d , μm	ρ , $\Omega \times \text{cm}$
1	60	315	2.5	0.12	90
2	30	270	2.56	0.06	50
3	30	375	2.58	0.06	0.5

This situation is explained by the fact that when spraying copper oxide II it decomposes in plasma and part of the oxygen is sprayed off by vacuum pumps. Moreover, the substrate temperature has a strong influence on the film parameters. Most likely with CuO RF magnetron sputtering, as a result, films of CuO _{x} ($0.5 \leq x \leq 1$) solid solutions are deposited.

The increase of the substrate temperature leads to the displacement of the stoichiometric composition of the film toward the Cu₂O ($x = 0.5$), which causes the increase of the band gap width. Reducing the oxygen content in the film results in an increase in the concentration of vacancies in the anionic sublattice, which increases the concentration of acceptors, and hence the electrical conductivity (Table 1). As evidenced by Table 1, larger (compared with other samples) resistance of sample 1 is associated, most likely, with longer duration of the spraying process, which can contribute to the recovery of vacancies in the anionic sublattice by the oxygen which is present in the plasma as a result of the decomposition of CuO during spraying.

3.2 Electrical Properties of Cu₂O/Cd_{1-x}Zn_xTe Heterostructure

The I - V -characteristics of the p -Cu₂O/ n -Cd_{1-x}Zn_xTe heterostructure (Fig. 3) were measured using a hardware-software system based on the Agilent 34410A digital multimeter and the Siglent SPD 3303 X power supply that were driven by a personal computer using the software created in LabView environment.

On the basis of the obtained I - V -characteristics, the extrapolation of the straight-line sections of the direct branches determined the value of the potential barrier height and obtained its temperature dependence (Fig. 3, inset) from which ϕ_0 (0 K) = 1.49 eV and the coefficient $B_\phi = 2.41 \times 10^{-3} \text{eV} \times \text{K}^{-1}$ were determined.

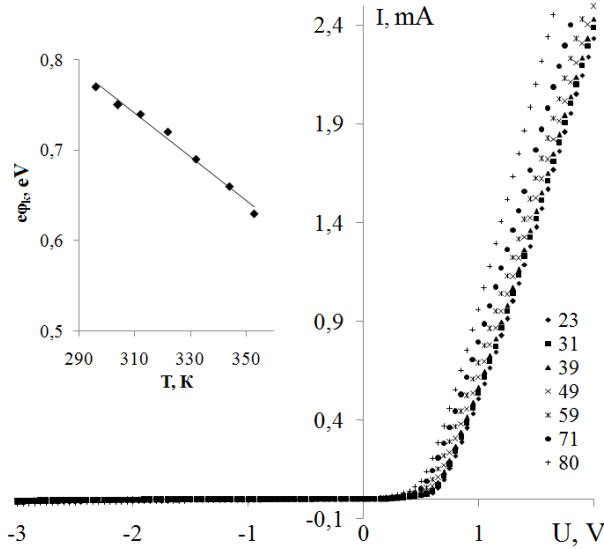


Fig. 3 – I - V -characteristics of $p\text{-Cu}_2\text{O}/n\text{-Cd}_{1-x}\text{Zn}_x\text{Te}$ at different temperatures; temperature dependence of the potential barrier height (inset)

From I - V -characteristics, the RR factor is determined for $|U| = 2$ V and $T = 296$ K and has a value of $RR \sim 10^3$ and decreases with increasing temperature. This is due to a decrease in the resistance of the base area with temperature ($\text{Cd}_{1-x}\text{Zn}_x\text{Te}$), (which confirms the temperature dependence of the series resistance (R_s)) (Fig. 4, inset), and as a consequence of the potential barrier height.

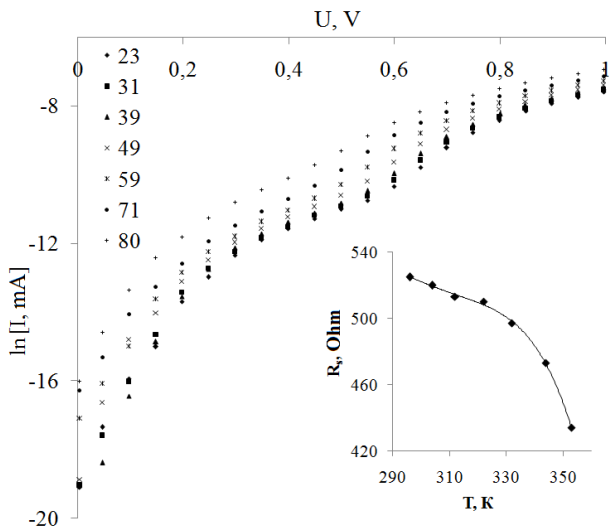


Fig. 4 – Direct branches of the I - V -characteristics of $p\text{-Cu}_2\text{O}/n\text{-Cd}_{1-x}\text{Zn}_x\text{Te}$ in half-logarithmic coordinates ($T = 300$ K); the temperature dependence of the series resistance (inset)

As seen from Fig. 4, on the dependences of the I - V -characteristics, which are constructed in semilogarithmic coordinates, there are observed rectilinear regions at

small ($0 \text{ V} < U < 0.2 \text{ V}$), medium ($0.2 \text{ V} < U < 0.5 \text{ V}$) and large ($0.5 \text{ V} < U < 0.7 \text{ V}$) displacements by means of which the indicator of nonideality of I - V -characteristics for each site is determined at each temperature. The obtained values are given in Table 2.

Table 2 – Indicator of nonideality of I - V -characteristics for $p\text{-Cu}_2\text{O}/n\text{-Cd}_{1-x}\text{Zn}_x\text{Te}$ heterostructure

T, K	296	304	312	322	332	344	353
small displacements ($0 < U < 0.2 \text{ V}$)	1.41	1.32	1.03	1.21	1.59	1.61	1.32
medium displacements ($0.2 \text{ V} < U < 0.5 \text{ V}$)	6.81	6.24	5.99	5.25	4.9	4.43	3.95
large displacements ($0.5 \text{ V} < U < 0.7 \text{ V}$)	3.48	3.43	3.5	3.59	3.5	3.5	3.95

The analysis of the obtained results (Table 2) showed that in the case of small displacements the over-barrier emission predominates; in the case of medium displacements, tunneling prevails, and at large displacements, the generation-recombination mechanism of current transfer with the participation of surface states on the metallurgical boundary separation. With increasing temperature, the generation-recombination mechanism of current transfer gradually disappears and passes into tunneling, which may be due to an increase in the concentration of electrons with a temperature rise in the base region of the heterojunction ($\text{Cd}_{1-x}\text{Zn}_x\text{Te}$) and a decrease in the potential barrier height.

The analysis of current transfer at inverse displacements showed that in the range of ($-1.2 \text{ V} < U < -0.2 \text{ V}$) the reverse current is described by the expression:

$$I'_{rev} \approx a_0 \exp\left(\frac{b_0}{\sqrt{\phi_0(T) - eV}}\right)$$

The dependence $\ln I = f(\phi_0 - qU)^{1/2}$ is a straight line (Fig. 5), which indicates that the tunneling mechanism of current transfer dominates at the indicated voltages.

At displacements ($U < -1.2 \text{ V}$), the Frenkel-Pul emission is observed, as evidenced by straight-line regions on the dependencies $\ln I = f(U^{1/2})$ (Fig. 5, inset).

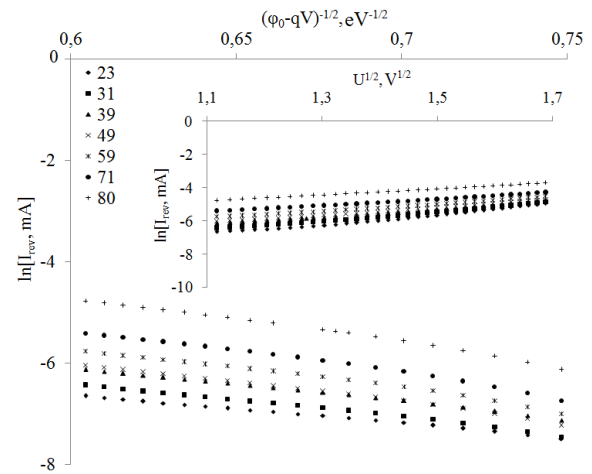


Fig. 5 – Reverse branches of the I - V -characteristics of $p\text{-Cu}_2\text{O}/n\text{-Cd}_{1-x}\text{Zn}_x\text{Te}$ in the case of tunneling mechanism of current transfer and Frenkel-Pul emission in the inset ($T = 300$ K)

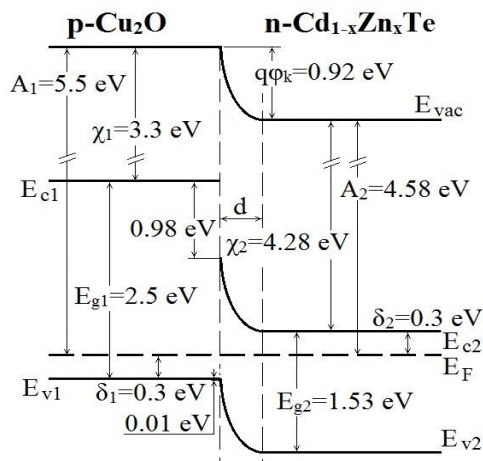


Fig. 6 – The energy diagram of the $p\text{-Cu}_2\text{O}/n\text{-Cd}_{1-x}\text{Zn}_x\text{Te}$ heterostructure in the thermodynamic equilibrium state ($T = 300\text{ K}$)

The essence of the processes occurring in this case consists in the relaxation of the electric field by the thermal excitation of charge carriers captured by surface traps [11]. The presence of a sufficiently strong electric field in the region of the heterojunction is confirmed by the high values of the contact potential difference (0.77 V at 296 K).

The energy diagram of the anisotropic heterostructures $p\text{-Cu}_2\text{O}/n\text{-Cd}_{1-x}\text{Zn}_x\text{Te}$ in accordance with the Anderson model, without taking into account the surface electrical states and the dielectric layer, was con-

structed based on the values of the energy parameters of the semiconductors (Fig. 6) [12, 13].

The values necessary to construct the energy diagram for $\text{Cd}_{1-x}\text{Zn}_x\text{Te}$ were determined experimentally, the affinity for an electron $\chi = 4.28\text{ eV}$ is taken as for cadmium telluride, for $p\text{-Cu}_2\text{O}$ it is determined from kinetic and optical studies (affinity for an electron for $\chi_{\text{Cu}_2\text{O}} = 3.3\text{ eV}$ is taken from [1]).

4. CONCLUSIONS

1. Cu_2O films with thicknesses of 60 and 120 nm were obtained using RF magnetron sputtering and different spraying modes, namely, changing the spraying time and the temperature of the substrates.

2. Optical studies have established the presence of direct permitted optical transitions and determined the optical width of the band gap of Cu_2O films (2.5-2.58 eV). Investigation of the electrical resistance of the films obtained showed that it reaches values of 0.5-90 $\Omega\cdot\text{cm}$, depending on the mode of application of thin films.

3. The $p\text{-Cu}_2\text{O}/n\text{-Cd}_{1-x}\text{Zn}_x\text{Te}$ heterostructure was obtained by applying the $p\text{-Cu}_2\text{O}$ films to $\text{Cd}_{1-x}\text{Zn}_x\text{Te}$ substrates. From the $I\text{-}V$ -characteristics of the heterostructure φ_0 (0 K) = 1.49 eV, the coefficient $B_\varphi = 2.41 \times 10^{-3}\text{ eV} \times \text{K}^{-1}$, and the factor $RR \sim 10^3$ ($|U| = 2\text{ V}$, $T = 296\text{ K}$) were determined. $I\text{-}V$ -characteristics constructed in semi-logarithmic coordinates allowed to determine the indicator of nonideality of $I\text{-}V$ -characteristics and to establish the dominant mechanisms of current transfer.

REFERENCES

1. J.-H. Guo, J.E. Cotter, *Prog. Photovoltaic*, **15**, 211 (2007).
2. T. Minami, Y. Nishi, T. Miyata, *J. Semiconductor*, **37**, 1674 (2016).
3. X. Liangbin, H. Sheng, Y. Xi, Q. Mingqiang, C. Zhenghua, Y. Ying, *Electrochimica Acta* **56**, 2735 (2011).
4. X. Mathew, N.R. Mathews, P.J. Sebastian, *Sol. Energ. Mat. Sol. C*, **70**, 277 (2001).
5. S. Ishizuka, T. Maruyama, K. Akimoto, *Jpn. J. Appl. Phys.* **39**, L786 (2000).
6. K. Guergouri, R. Triboulet, A. Tromson-Carli, Y. Marfaing, *J. Cryst. Growth* **86**, 61 (1988).
7. I.P. Kozziarskyi, E.V. Maistruk, D.P. Kozziarskyi, P.D. Maryanchuk, *Inorg. Mater.* **50**, 447 (2014).
8. I.P. Kozziarskyi, S.L. Abashin, E.V. Maistruk, P.D. Marianchuk, D.P. Kozziarskyi, Y.A. Yatsina, *J. Surf. Investig.-X-Ray*, **9**, 415 (2015).
9. E.V. Maistruk, P.D. Mar'yanchuk, M.N. Solovan, F. Pinna, E. Tresso, *Opt. Spectrosc.* **123**, 38 (2017).
10. I.P. Kozziarskyi, E.V. Maistruk, D.P. Kozziarskyi, P.D. Maryanchuk, *J. Nano-Electron. Phys.* **10**, 01028 (2018).
11. S.M. Sze, K.N. Kwok, *Physics of semiconductor devices* (Wiley: 2007).
12. A. Luque, S. Hegedus, *Handbook of photovoltaic science and engineering* (Hoboken, NJ: John Wiley & Sons: 2011).
13. J. Franc, P. Hlídaek, P. Moravec, E. Belas, P. Höschl, L. Turjanska, R. Varghová, *Semicond. Sci. Tech.* **15**, 561 (2000)

Електричні властивості гетероструктури $\text{Cu}_2\text{O}/\text{Cd}_{1-x}\text{Zn}_x\text{Te}$

Е.В. Майструк, І.П. Козьярський, Д.П. Козьярський, П.Д. Мар'янчук

Чернівецький національний університет імені Юрія Федьковича,
вул. Коцюбинського 2, 58012 Чернівці, Україна

У роботі досліджено вплив умов вирощування на оптичні та електричні властивості тонких плівок Cu_2O . Також досліджено електричні властивості гетероструктури $p\text{-Cu}_2\text{O}/n\text{-Cd}_{1-x}\text{Zn}_x\text{Te}$ отриманої на основі цих плівок.

Тонкі плівки Cu_2O отримували методом ВЧ-магнетронного розпилення мішені з порошку оксиду міді II на підкладки зі скла та ситалу. При одержанні досліджуваних плівок змінювали температуру підкладок ($270^\circ\text{C} \leq T_s \leq 375^\circ\text{C}$) та час розпилення мішені ($30\text{ хв} \leq t \leq 60\text{ хв}$). При оптимальних режимах були отримані плівки $p\text{-Cu}_2\text{O}$ із шириною оптичної забороненої зони $E_g^{\text{opt}} = 2,6\text{ eV}$ та питомим опором $\rho = 0,5\text{ Ом} \times \text{см}$. Методом ВЧ магнетронного розпилення мішені з порошку оксиду міді II на свіжо сколоті підкладки $\text{Cd}_{1-x}\text{Zn}_x\text{Te}$ були отримані гетероструктури $p\text{-Cu}_2\text{O}/n\text{-Cd}_{1-x}\text{Zn}_x\text{Te}$. Дослідження впливу температури ($23^\circ\text{C} \leq T \leq 80^\circ\text{C}$) на ВАХ гетероструктур $p\text{-Cu}_2\text{O}/n\text{-Cd}_{1-x}\text{Zn}_x\text{Te}$ показали, що гетероструктури володіють яскраво вираженим випрямляючим ефектом із коефіцієнтом випрямлення $RR \sim 10^3$ при напрузі

2 В, висота потенціального бар'єру $e_{ph} = 0.77$ еВ при $T = 296$ К та зменшується з ростом температури. Послідовний опір гетероструктур сягає $R_s \sim 500$ Ом при кімнатній температурі формується підкладкою $n\text{-Cd}_{1-x}\text{Zn}_x\text{Te}$ і зменшується з ростом температури. Дослідження механізмів струмопереносу показали, що при малих зміщеннях переважає надбар'єрна емісія, при середніх – тунелювання, а при великих – генераційно-рекомбінаційний механізм струмопереносу за участю поверхневих станів на металургійній межі поділу. При підвищенні температури генераційно-рекомбінаційний механізм струмопереносу поступово зникає і переходить в тунелювання, що може бути пов'язане із ростом концентрації електронів з температурою у базовій області гетеропереходу ($\text{Cd}_{1-x}\text{Zn}_x\text{Te}$) та зменшенням висоти потенціального бар'єру.

Ключові слова: Тонкі плівки, Гетероструктура, ВАХ, Cu_2O , ВЧ-магнетронне напылення.